The Compatibility of Acyclovir with Polyacrylonitrile in the Electrospun Drug-Loaded Nanofibers

Deng-Guang Yu,[1] Christopher Branford-White,[2] Lan Li,[3] Xiao-Mei Wu,[1] Li-Min Zhu[1]

[1]*College of Chemistry, Chemical Engineering and Biotechnology, Donghua University, Shanghai 201620, China*
[2]*Institute for Health Research and Policy, London Metropolitan University, London N7 8DB, United Kingdom*
[3]*Center of Analysis, Measurement of Donghua University, Shanghai 201620, China*

Received 16 May 2009; accepted 20 December 2009
DOI 10.1002/app.32019
Published online 29 March 2010 in Wiley InterScience (www.interscience.wiley.com).

ABSTRACT: Drug delivery systems (DDS) derived from drug-loaded fibers have attracted increasing attention in recent years. In this study, drug-loaded nanofibers with varying drug-to-polymer ratios were prepared using electrospinning with acyclovir (ACY) as the model drug and polyacrylonitrile (PAN) as the filament-forming matrix polymer. The compatibility of ACY with PAN was investigated by FTIR, DSC, XRD, and morphological studies. The obtained results clearly demonstrated that ACY had good compatibility with PAN and was able to be evenly distributed in the polymer fiber matrix. ACY present in the drug-loaded fibers with a drug content of 10 wt % was in an amorphous state. As the ACY contents in the fibers increased up to 20 wt % drug crystals began to form and ACY separated from the fiber matrix. FTIR results illustrated that the main interactions between PAN and ACY was hydrogen bonding and data from ^{1}H-NMR showed that ACY was able to retain its chemical integrity during the electrospinning. All the fibers with varying drug content provided sustained drug release profiles over a 12-h period. The drug-loaded fibers prepared in this study could provide new approaches for developing novel transdermal DDS or skin topical DDS. © 2010 Wiley Periodicals, Inc. J Appl Polym Sci 117: 1509–1515, 2010

Key words: compatibility; electrospinning; drug-loaded nanofibers; acyclovir; ploy acrylonitrile; drug delivery systems

INTRODUCTION

Textiles and fibers used for medical and hygiene purposes have a long history and are still used. Sutures and wound dressings are examples of commonly applied to fiber-based medical devices. Transdermal patches and ion-exchange fibers containing therapeutic ingredients for delivering have become commonplace.[1,2] Along with developments in other relative disciplines such as polymer sciences, medicines and pharmaceuticals, textile technologies, such as wet and dry spinning, melt spinning and electrospinning have enhanced and expanded drug application opportunities in pharmaceutics.[3–7]

Electrospinning is a simple and versatile process by which polymer nanofibers with diameters ranging from a few nanometers to several micrometers can be produced using an electrostatically driven jet of polymer solution or polymer melt. Since 1980s and especially in recent years, the electrospinning process has regained more attention probably due in part to a surging interest in nanotechnology, as ultrafine fibers or fibrous structures of various polymers with diameters as low as submicrons or nanometers can be easily fabricated. Furthermore, over the past few years significant progress has been made and in particular the development of electrospun nanofibers and these are of interest in pharmaceutics.[8–11]

The use of DDS from electrospun nanofibers formed as nonwoven mats has gradually gained interest since the early work of Kenawy et al.[12] Recent reports have demonstrated that DDS based drug-loaded nanofibers could be applied as transdermal DDS, oral sustained DDS, targeted DDS, implantable DDS, DDS for tissue engineering, and trans-membrane DDS.[13–16] It is well known that the compatibility of drugs with the filament-forming matrix polymers is vital for successfully preparing drug-loaded fibers. Often the compatibility of the drug with the carrier polymer influences the properties of nanofibers such as drug loading capability, drug distributions and existing state (microcrystal, amorphous, particles), mechanical performance and the corresponding drug release controllability.[17,18] Currently polymeric nanofibers acting as novel carriers for the delivery of therapeutic molecules have drawn more attentions,[19] however, detailed

Correspondence to: L.-M. Zhu (lzhu@dhu.edu.cn).
Contract grant sponsor: UK-CHINA Joint Laboratory for Therapeutic Textiles and Biomedical Textile Materials.
Contract grant sponsor: China Postdoctoral Science Foundation; contract grant number: 200902195.

© 2009 Wiley Periodicals, Inc.

information about compatibility factors influencing the polymer matrix and loaded therapeutic molecules remain very limited.

Acyclovir (ACY) is one of the most effective and selective antiviral drugs and is commonly used for the treatment of herpes viruses (include the human milk head lump virus, herpes simplex virus, and cytomegalovirus) that could cause gynecological diseases.[20] Compared to oral DDS, transdermal DDS has the advantages that includes ease of use, relatively safe and the process can interrupted by simple removal of the skin overdosing is suspected. Thus transdermal DDS of ACY are often reported in literatures.[21,22] On the other hand, polyacrylonitrile (PAN) is a polymer that has good filament-forming properties and is the precursor for high-performance carbon fiber. PAN-based composite fibers are light, flexibility and can be easily molded. Many research groups have worked on fabricating PAN-based functional fibers through incorporating other materials such as TiO_2, AgCl, and silica.[23–25]

In this study, ACY-loaded PAN nanofiber membrane which have the potential for preparing transdermal DDS and skin topical DDS were prepared using electrospinning and the compatibility of ACY with PAN were investigated in detail.

EXPERMENTAL

Materials

Polyacrylonitrile (PAN) powders (with an average molecular weight of 80,000) were purchased from Jinshan Petrochemistry (Shanghai, China). ACY was purchased from Zhejiang Charioteer Pharmaceutical Company. The spinning solvent *N*,*N*-dimethyl foramide (DMF) and dimethyl sulfoxide (DMSO) were provided by the Sinopharm Chemical Reagent. All other chemicals used were analytical grade, and water was distilled just before use.

Preparation of spinning solutions

The codissolving method was employed to prepare the drug-loaded spinning solvent system. The PAN powder was dried in the DZF-6050 Vacuum Oven (Shanghai Laboratory Instrument Work, Shanghai, China) to minimize the effect of moisture absorption on the content of PAN. Three spinning solutions were prepared with the ratios of ACY to PAN in the final electrospun nanofibers were 1 : 9, 2 : 8, and 3 : 7, and correspondingly the fibers were denoted as F1, F2, and F3, respectively. In all the three solutions, the concentration of PAN was fixed at 8 wt %.

The mixed solvent of DMF to DMSO with a ratio of 70 : 30 by weight was used to prepare the spinning solutions. After ACY was added to the solvent and fully dissolved the PAN powder was added into the solution to dissolve at 70°C under quickly stirring. The codissolved spinning solution was cooled to ambient temperature and degassed with a SK5200H ultrasonator (Shanghai Jinghong Instrument, Shanghai, China) for 15 min before electrospinning processes.

Electrospinning process

A high voltage power supply (Shanghai Sute Electrical) was used to provide high voltages in the range of 0–60 kV. To avoid carrying air bubbles spinning solutions were carefully loaded using a 10-mL syringe which contained a stainless steel capillary metal-hub needle, the internal diameter of the needle being 0.5 mm. The positive electrode of the high voltage power supply was connected to the needle tip while the grounded electrode was connected to a metal collector wrapped with aluminum foil.

Electrospinning was carried out at room conditions (Temperature was 21 ± 1°C and relative humidity was 71 ± 3%). A fixed electrical potential of 12 kV was applied across a fixed distance of 15 cm between the tip and the collector. The feed rate of solutions was controlled at 2.0 mL h^{-1} by mean of a single syring pump (Cole-Parmer®). The formed fibers were allowed to be further dried for over 24 h at 40°C and under vacuum (320 Pa) in a DZF-6050 Electric Vacuum Drying Oven (Shanghai Laboratory Instrument, Shanghai, China) to facilitate the removal of residual organic solvent.

Characterization

The surface morphology of the electrospun fibers were assessed using a JSM-5600LV scanning electron microscope (Japan Electron Optics Laboratory). Prior to the examination, the samples were gold sputter-coated under argon atmosphere to render them electrically conductive. The pictures were then taken at an excitation voltage of 15 kV.

The wide-angle X-ray diffractograms (XRD) were obtained on a D/Max-BR diffractometer (RigaKu, Japan) with Cu Kα radiation in the 2q range of 5–60° at 40 mV and 300 mA.

The differential scanning calorimetry (DSC) analyzes were carried out using an MDSC 2910 differential scanning calorimeter (TA Instruments). Sealed samples were heated at 10°C /min from 50 to 300°C. The nitrogen gas flow rate was 40 mL/min.

Fourier-transform infrared (FTIR) was obtained on a Nicolet-Nexus 670 FTIR spectrometer (Nicolet Instrument Corporation, Madison) using the KBr disk method (2 mg sample in 200 mg KBr). The scanning range was 500–4000 cm^{-1} and the resolution was 2 cm^{-1}. In all the experiments, physical

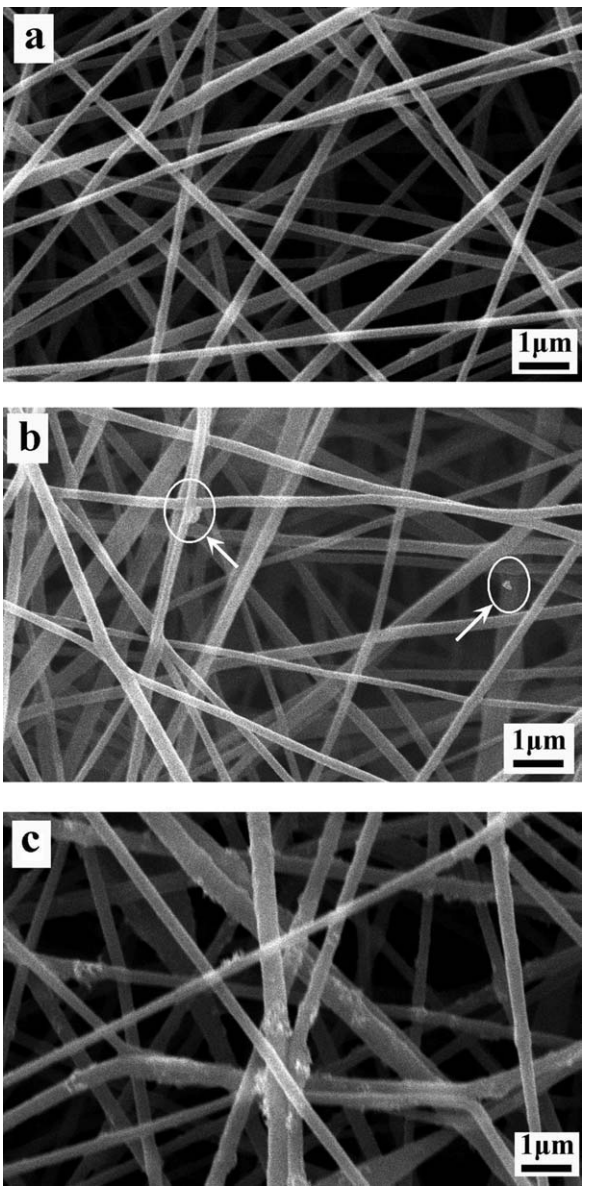

Figure 1 Drug-loaded fibers' SEM images, (a) F1, (b) F2, (c) F3. As the drug loading increased, more particles were released from the PAN fiber matrix.

mixtures (PM) of ACY and PAN powders with a mass ratio of 2 : 8 were used as control.

A ^{1}H-NMR spectrometer (Bruker DRX 400MHz NMR spectrometer, Germany) was used to investigate the chemical stability of the loaded ACY during electrospinning using deuterated dimethylsulfoxide (DMSO-d_6) as solvent.

The *in vitro* dissolution tests were conducted using a ZRS-8G dissolution tester (Tianjin, China) based on the Chinese Pharmacopoeia Method (paddle method). Samples containing about 50 mg of ACY were immersed in 900 mL of distilled water thermostatically maintained at 37 ± 0.1°C at a rotation rate of 100 rpm, sink conditions $C < 0.2C_s$. At appropriate time intervals samples (5 mL) were withdrawn and filtered (Millipore, 0.22 μm). The filtrate was analyzed at 257 nm by a UV spectrophotometer (Unico Instrument, Shanghai, China). A calibration curve was constructed from reference standards that was used to determine the cumulative amount of ACY released from the specimens at each time interval. All the experiments were carried out in triplicate.

RESULTS AND DISCUSSION

Preparation

Solvent selection is often a key factor in determining both the ability of polymer solutions to undergo electrospinning and the structural homogeneity of the nanofibers.[26] In preparing composite nanofibers from codissolving solutions of polymer and the functional materials using electrospinning the solvent selection is critically important as it influences the properties of the polymer solutions and the solubility of the additive must be taken into account.

From traditional wet-spinning experiments, the organic solvents that are suitable for preparing PAN fibers are dimethyl sulfoxide (DMSO), *N*,*N*-dimethyl acetamide (DMAc), and *N*,*N*-dimethyl formamide (DMF). All the solvents have relatively high boiling points and elevated temperatures for electrospinning have been reported for preparing PAN nanofibers.[27] Among the three solvents, DMF has the lowest boiling point which implies that it is the most suitable candidate for preparing PAN fibers for electrospinning. However, ACY exhibits an order of solubility in the three solvents: DMSO > DMAc > DMF. Thus, based on aforementioned factors and pre-experiments, we found that a mixed solvent of DMF:DMSO with a ratio of 70 : 30 by volume was found to be the most appropriate mix for spinning the codissolving solutions of ACY and PAN into composite nanofibers.

The codissolving solutions of PAN and ACY in the mixed solvent of DMF and DMSO was semitransparent and in a bright yellow color.

Morphology

The configuration of the drug-loaded fibers is shown in Figure 1. All fibers had a similar diameter within the range 400–600 nm and it should be noted that several drug particles could be seen in Figure 1(b) on the drug-loaded fibers separated out during electrospinning. More particles were shown in Figure 1(c) but none were apparent [Fig. 1(a)]. It can be presumed that the drug was in an aggregated form and this being due to hydrogen bonding under the surface tensions and shear forces that formed during the electrospinning when the drug content in the codissolving solutions increased. Thus, the ratios of

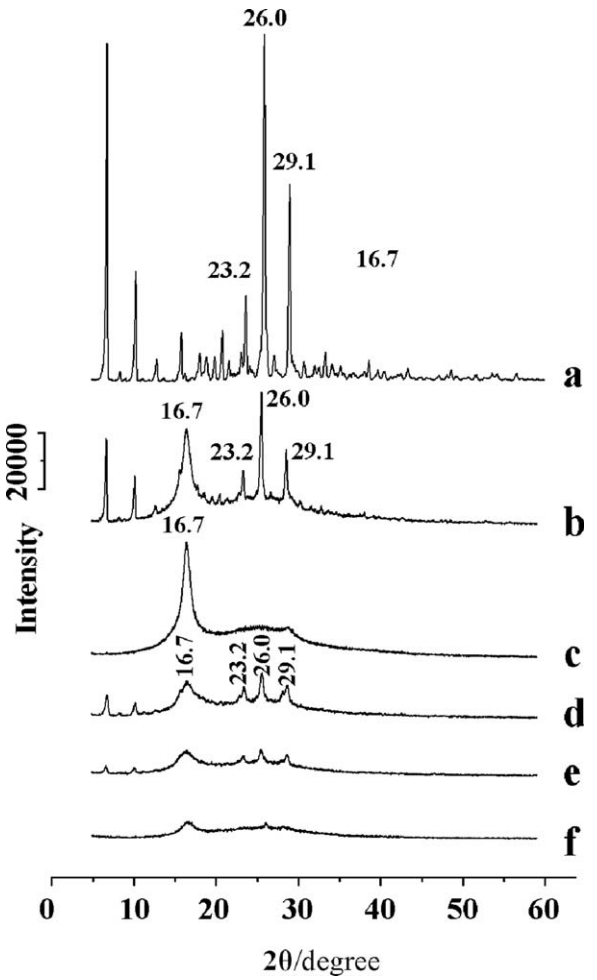

Figure 2 X-ray diffraction patterns: a-ACY, b-PM, c-PAN, d-F3, e-F2, f-F1. As the drug loading increased, the characteristic diffraction of crystalline ACY in the nanofibers appeared became more intense.

drug-to-PAN has influenced the morphological structure of the drug-loaded nanofibers and at higher ACY content resulted in the formation of crystalline structures which often influenced drug distribution uniformity in the matrix and hence the drug release profiles.

XRD analysis

The presence of numerous distinct peaks [Fig. 2(a)] in the X-ray diffraction patterns indicated that ACY was present as a crystalline material with characteristic diffraction peaks appearing at a diffraction angle of 2θ at 23.2, 26.0, 29.1 degree. The pattern of PAN [Fig. 2(c)] was characterized by characteristic diffraction peaks appearing at a diffraction angle at 16.7 degree.

Compared with the pure ACY particles and PAN powders the PM [Fig. 2(b)] had the same characteristic peaks and when superposed the peaks had almost the intensities implying there was no interaction between PAN and ACY in the mixed powder states.

Compared with the pure ACY particles, PAN powders and also the PM, diminution intensity of both ACY and PAN peaks were distinct in the diffraction patterns of the three drug-loaded fibers. In Figure 2(f), the characteristic peaks of ACY had almost disappeared with only a minute peak appearing at an angle 26.0 degree. Similarly, the characteristic peak of PAN was also small suggesting that interactions between PAN and ACY had created a transition from crystalline material to a polymer-drug complex that was in an amorphous form. As the drug content increased in the composite fibers, the intensity of characteristic peaks of ACY and PAN increased synchronously, illustrating that more crystals were formed and separated out in the fiber matrix. These results concurred with those obtained from the morphological observations.

Differential scanning calorimetry analysis

All DSC thermograms are shown in Figure 3. The DSC curve of pure ACY [Fig. 3(a)] exhibited a single endothermic response corresponding to the melting of the acyclovir at 257.1°C (ΔH_f 162.6 J/g). The profile for PAN [Fig. 3(f)] did not demonstrate any fusion peak or phase transition before it decomposed at peak temperature around 300°C.

DSC thermograms of nanofibers F1 [Fig. 3(d)] did not give a melting peak of ACY thus indicating that all incorporated drug was converted into an amorphous state. Whereas the nanofibers F2 and F3 [Fig. 3(b,c)] had small melting peaks for ACY, showing that there were some ACY crystals in the nanofibers when the drug content increased to 20 wt %, At this concentration the endotherms broadened and the peak temperatures were shifted to the lower temperatures (216.3 and 222.4°C) reflecting changes of ACY crystal structure.

For the PM [Fig. 3(e)], the endotherms were almost the same as those superposed from ACY and PAN, except the peak temperatures of acyclovir melting and PAN decomposition were shifted slightly to lower temperatures (255.4 and 287.6°C) so implying there was no interaction between PAN and ACY.

FTIR analysis

The FTIR spectra of PAN, ACY, PM, and the drug-loaded fibers are shown in Figure 4. The existence of ACY and PAN in the drug-loaded nanofibers was confirmed by characteristic absorption bands at 1696 cm^{-1} (—C=O) and 2243 cm^{-1} (—C≡N—).

Comparison of the spectra of drug-loaded nanofibers at different levels of ACY demonstrated the - relative intensity of the three wave peaks occurring between 1500 and 1750 $cm^{-1.}$ As the drug

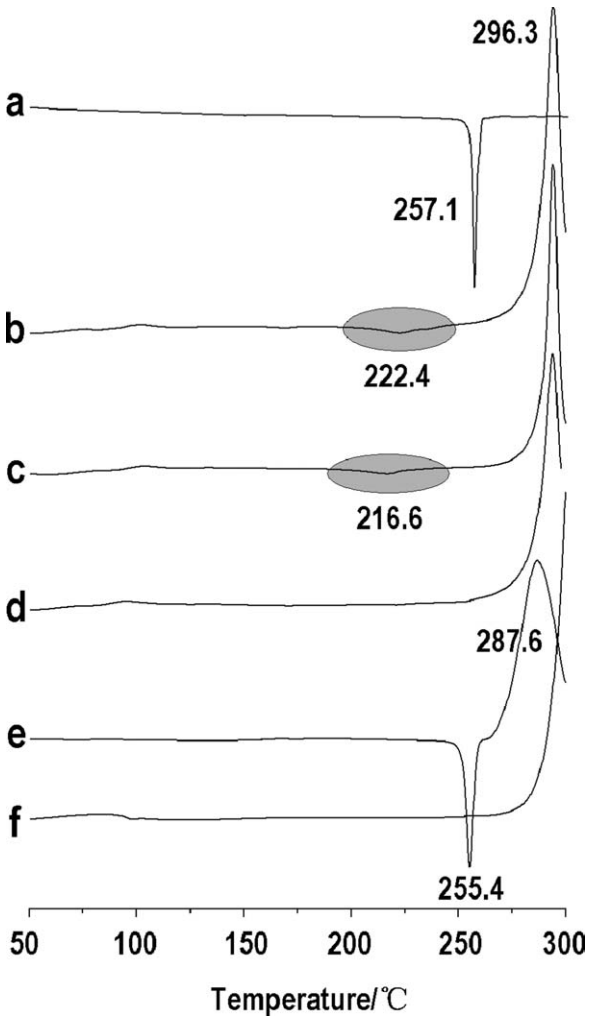

Figure 3 DSC thermograms: a-ACY, b-F3, c-F2, d-F1, e-PM, f-PAN. As the drug loading increased, the melting peak of ACY crystals in the nanofibers appeared and enlarged.

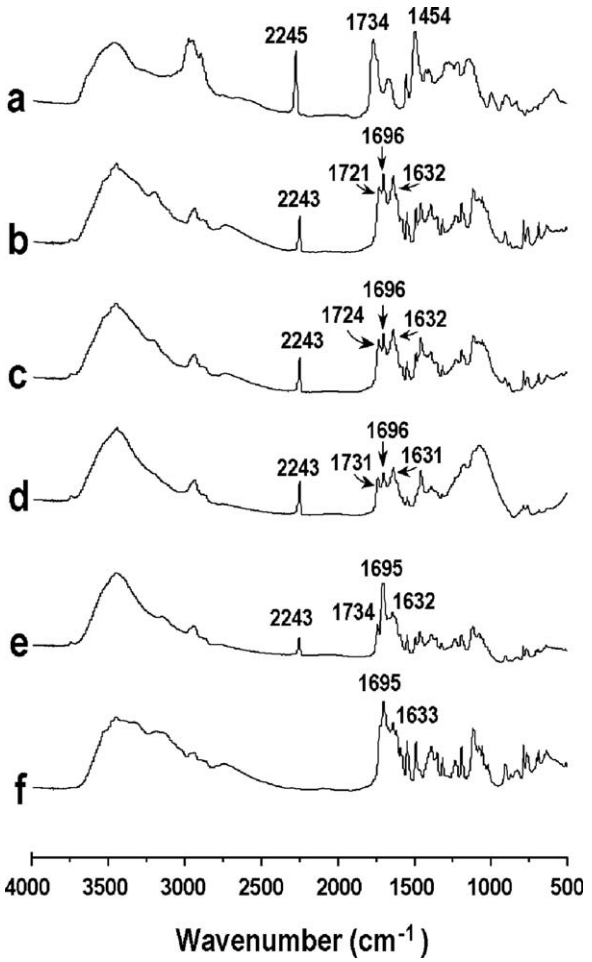

Figure 4 FTIR spectra, a-PAN, b-F3, c-F4, d-F5, e-PM, f-ACY.

concentration increased the first peaks in this region diminished and shifted to a lower wave-number (1731 to 1724 and to 1721). This observation supports the view that bending vibration of —C≡N weakened due to the formulation of hydrogen bonding between —C≡N of PAN and —OH of the ACY molecules [Fig. 5(b)], whereas the intensity of 1696 cm^{-1} augmented gradually as the concentrations of ACY in the nanofibers increased.

It is postulated that when the ratio of drug-to-PAN is reduced, both ACY and PAN were able to interact and that ACY was distributed in the drug-loaded fibers as an amorphous solid form and as an outcome almost no drug particles appeared on the surface of the fibers. However, when the ratio of drug-to-PAN increased hydrogen bonding occurred between the ACY molecules during electrospinning [Fig. 5(a)] and so the formed drug particles separated out from the fiber matrix. The higher the content of ACY in the spinning solutions resulted in more the drug particles being visible on the nanofiber surfaces. These results agree with the conclusions drawn from morphological observations.

The stability of ACY at electrical potential during the electrospinning is crucial to the effectiveness of the drug as an active pharmaceutical agent. To verify this, drug-loaded electrospun fibers were dissolved in DMSO-d_6 and solutions were investigated

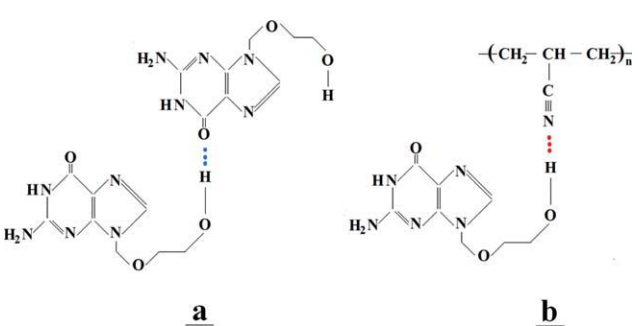

Figure 5 Hydrogen bonding, (a) between two ACY molecules, (b) between ACY and PAN molecule. [Color figure can be viewed in the online issue, which is available at www.interscience.wiley.com.]

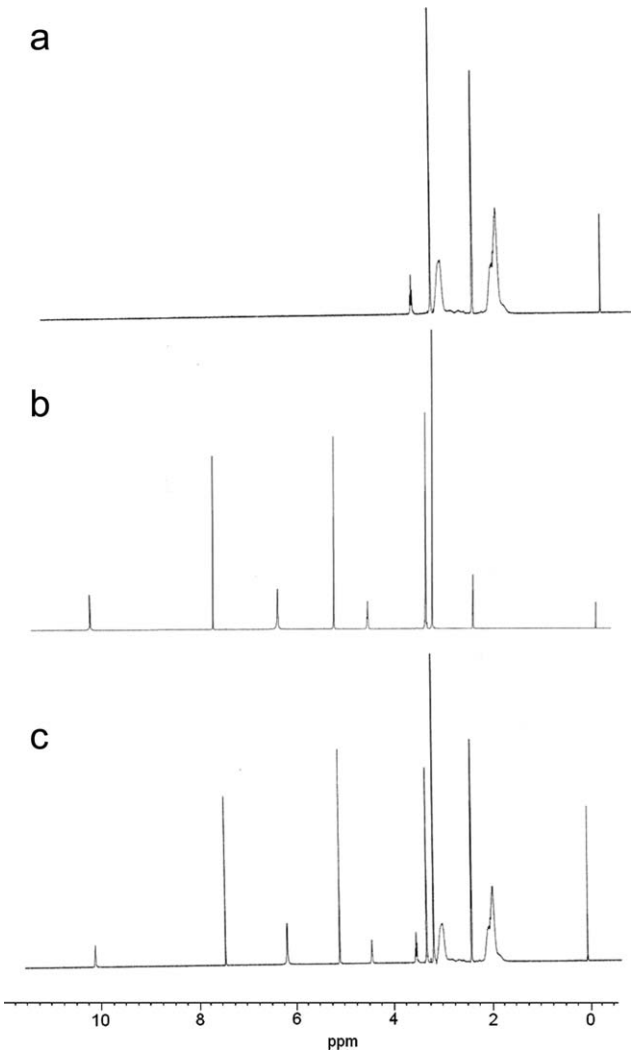

Figure 6 1H-NMR spectrums of PAN (a), ACY (b), and fiber F3 (c) in solutions containing 5 wt % of the solutes in DMSO-d_6. The peaks corresponding to PAN and ACY could be observed in the ^{1}H-NMR spectrum of the drug-loaded fiber mats so indicating that the chemical integrity of the as-loaded-ACY was sustained after the electrospinning.

by ^{1}H-NMR with solutions of both the drug-free PAN electrospun fibers and pure ACY in DMSO-d_6 being used as references. ^{1}H-NMR spectrum of the drug, drug-free PAN fibers and the drug-loaded fibers are shown (Fig. 6) and the spectra were obtained from a solution containing 5 wt % of solute. Evidently, the chemical integrity of the as-loaded-ACY was sustained after the electrospinning as the peaks corresponding to both PAN and ACY could be observed in the ^{1}H-NMR in the drug-loaded fiber mat spectra.

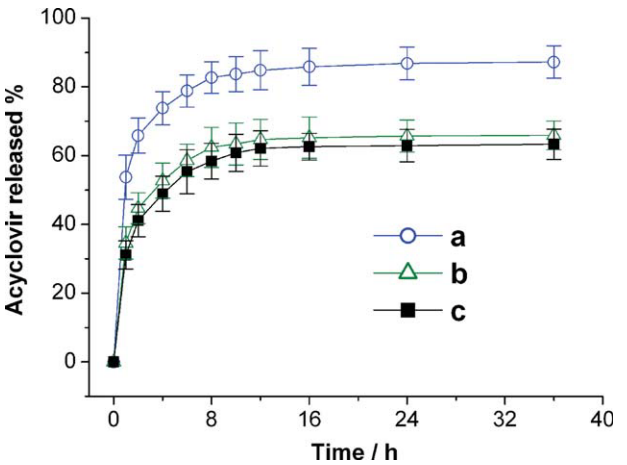

Figure 7 Accumulative release profiles of ACY *in vitro* from fibers F3-a, F2-b and F1-c. [Color figure can be viewed in the online issue, which is available at www.interscience.wiley.com.]

ACY release profiles from electrospun fiber mats with different drug-to-PAN ratios are given in Figure 7. All the fibers could provide a sustained release profiles over a time periods over 12 h and overall the drug release curves were similar. However initial burst release characteristics showed gradual release of the drug and this reached a plateau after a given time.

As indicated in Table I, the initial burst release effect was evident for the three fibers. In the first hour, 31.12, 33.67, and 52.74% of the loading ACY was released from the fibers F1, F2, and F3, respectively. Higher drug loading increased the initial burst effects, as indicated by F3. The separated ACY particles facing the fibers surface appear to account for this phenomenon. The initial release effect of

TABLE I
ACY Release Profiles from Nanofibers with Different ACY-to-PAN Ratios

Fiber	ACY to PAN Ratio	R_{ACY} in the first hour (%)[a]	R_{ACY} after 36 h (%)	Regressed equation[b]	
				Peppas equation	R^2
F1	10:90	31.12	63.23	$Q = 1.52\ t^{0.2718}$	0.9853
F2	20:80	33.67	66.96	$Q = 1.55\ t^{0.2593}$	0.9786
F3	30:70	52.74	88.22	$Q = 1.74\ t^{0.1869}$	0.9738

[a] R_{ACY} denotes accumulative release of ACY in percentage.
[b] Regressed equation denotes that the equations were regressed according to the Peppas equation from the acyclovir release data before 12th h when the release curve reached optimum levels.

fibers F1 and F2 appear to be due to the large surface area of the fibers and the dispersal of drug on the fiber surface and this would facilitate the drug being dissolved into the dissolution medium. However, the less the drug contained within the fibers the of the larger amount of ACY being encapsulated by PAN and this would be exhausted in the test time periods.

It can be concluded from *in vitro* release profiles of ACY were suboptimal. However the drug-loaded fibers still provide a system for developing novel transdermal DDS or skin topical DDS as there is sustained release effect occur over 12 h.

To further assess the release mechanism of ACY-loaded nanofiber mats the Korsmeyer–Peppas equation (see below) was used to describe the drug release behavior from polymeric systems.[28]

$$Q = k \times t^n \quad \text{or} \quad 1\text{g}Q = n \times 1\text{g}t + k_0$$

where Q is the drug release percentage and t is the release time, k is a constant incorporating the structural and geometric characteristics of fibers and n is the release exponent indicative of the drug release mechanism. The kinetic parameters (n and k) were calculated from the plot of log Q versus log t where $t \leq 12$ h.

The n values given in Table I, fibers F1, F2, and F3 had a value of 0.2718, 0.2593, and 0.1869, respectively. These results suggest that acyclovir has similar diffusion properties regardless of the drug loading capacity. The threshold of n value between Fickian and non-Fickian mechanism was 0.45.[29] All the release profiles tested in this study were calculated using the aforementioned equation and no value above 0.45 was determined. This confirms that the release mechanism of ACY from the fibers is fits a typical Fickian diffusion.

CONCLUSIONS

ACY-loaded PAN nanofibers with varying drug-to-polymer ratios have been successfully prepared using electrospinning. The results from XRD, DSC and SEM demonstrate that ACY had good compatibility with PAN and was able to distributed evenly within the polymer fiber matrix. ACY present in the drug-loaded fibers with a drug content of 10 wt % was in an amorphous state, different with pure drug and physical mixture of PAN and ACY. As the ACY contents in the fibers increased (up to 20 wt %) crystals of the drug began to form and these separated out from the fiber matrix. FTIR results illustrated that the interactions between PAN and ACY occurred through hydrogen bonding between the —C≡N of PAN molecules and —OH of ACY. ^{1}H-NMR spectrum demonstrated that ACY was able to keep it chemical integrity during the electrospinning process. Irrespective of there drug content all loaded fibers could provide a sustained drug release profile over 12 h. As the drug contents increased the initial burst release effect was more apparent. Although the *in vitro* release profiles were suboptimal, the drug-loaded fibers did exhibit potential for developing novel transdermal DDS or skin topical DDS.

References

1. Ma, Z. H.; Yu, D. G.; Branford-White, C. J.; Nie, H. L.; Zhu, L. M. Colloids Surf B: Biointerfaces 2009, 69, 85.
2. Zilberman, M. Acta Biomater 2007, 3, 51.
3. Nie, H. L.; Ma, Z. H.; Fan, Z. X.; Branford-White, C. J.; Ning, X.; Zhu, L. M.; Han, J. Int J Pharm 2009, 373, 4.
4. Zhang, X. F.; Yu, D. G.; Zhu, S.; Shen, X. X.; Branford-White, C. J.; Zhu, L. M. J Text Res 2009, 30, 1.
5. Yu, D. G.; Shen, X. X.; Zheng, Y.; Ma, Z. H.; Zhu, L. M.; Branford-White, C. J. In The 2nd International Conference on Bioinformatics Biomedical Engineering; IEEE Computer Society: New Jersey, 2008; p 1375.
6. Yu, D. G.; Shen, X. X.; Zhang, H. T.; Branford-White, C. J.; Zhu, L. M. J Biotech 2008, s431.
7. Zhu, S. J.; Yu, D. G.; Zhu, L. M.; Branford-White, C. J. In The 2nd International Conference on Bioinformatics Biomedical Engineering; IEEE Computer Society: New Jersey, 2008; p 1379.
8. Qin, X. H.; Yang, E. L.; Li, N.; Wang, S. Y. J Appl Polym Sci 2007, 103, 3865.
9. Son, B.; Yeom, B. Y.; Song, S. H.; Lee, C. S.; Hwang, T. S. J Appl Polym Sci 2009, 111, 2892.
10. Du, J.; Zhang, X. J Appl Polym Sci 2008, 109, 2935.
11. Wang, T.; Kumar, S. J Appl Polym Sci 2006, 102, 1023.
12. Kenawy, E. R.; Bowlin, G. L.; Mansfield, K.; Layman, J.; Simpson, D. G.; Sanders, E. H.; Wnek, G. E. J Controlled Release 2002, 8, 57.
13. Wang, M.; Wang, L.; Huang, Y. J Appl Polym Sci 2007, 106, 2177.
14. Rutledge, G. C.; Vfridrikh, S. Adv Drug Deliv Rev 2007, 59, 1384.
15. Still, T. J.; Von Recum, H. A. Biomaterials 2008, 29, 1.
16. Yu, D. G.; Shen, X. X.; Branford-White, C.; White, K.; Zhu, L. M.; Bligh, S. W. A. Nanotechnology 2009, 20, 055104.
17. Verreck, G.; Chun, I.; Peeters, J.; Rosenblatt, J.; Brewster, M. E. Pharm Res 2003, 20, 810.
18. Zeng, J.; Yang, L.; Liang, Q. Z.; Zhang, X. F.; Guan, H. L.; Xu, X. L.; Chen, X. S.; Jing, X. B. J Controlled Release 2005, 105, 43.
19. Kumbar, S. G.; Nair, L. S.; Bhattacharyya, S.; Laurencin, C. T. J Nanosci Nanotechnol 2006, 6, 2591.
20. Baker, D. A. Int J Fertil 1999, 44, 227.
21. Xu, Q.; Ibrahim, S.; Higuchi, W. I.; Li, S. K. Int J Pharm 2009, 369, 105.
22. Hu, O. Y. P. U.S. Pat. 6,162,459 (2000).
23. Kedem, S.; Schmidt, J.; Paz, Y.; Cohen, Y. Langmuir 2005, 21, 5600.
24. Bai, J.; Li, Y. X.; Yang, S. T.; Du, J. S.; Wang, S. G.; Zhang, C. Q.; Yang, Q. B.; Chen, X. S. Nanotechnology 2007, 18, 305601.
25. Ji, L.; Zhang, X. Mater Lett 2007, 62, 2161.
26. Li, D.; Xia, Y. Adv Mater 2004, 16, 1151.
27. Wang, C.; Chien, H. S.; Hsu, C. H.; Wang, Y. C.; Wang, C. T.; Lu, H. A. Macromolecules 2007, 40, 7973.
28. Limmatvapirat, S.; Limmatvapirat, C.; Puttipipatkhachorn, S.; Nunthanid, J.; Luangtana-Anan, M.; Sriamornsak, P. Eur J Pharm Biopharm 2008, 69, 1004.
29. Gao, H.; Gu, Y.; Ping, Q. J Controlled Release 2007, 118, 325.